

Role of the dihedral angle potential in the nucleation pathway of protein folding

Y. S. Djikaev*

Department of Chemical and Biological Engineering, SUNY at Buffalo,
Buffalo, New York 14260

(Received

Abstract.

A kinetic model for the nucleation mechanism of protein folding is proposed. A protein is modeled as a heteropolymer consisting of hydrophobic and hydrophilic beads with equal constant bond lengths and bond angles. The total energy of the heteropolymer is determined by the repulsive/attractive interactions of non-linked beads and the contribution from the dihedral angles involved. Their parameters can be rigorously defined, unlike the ill defined surface tension of a cluster of protein residues which is the basis of the previous model. As a crucial idea of the model, the dihedral potential in which a selected bead is involved is averaged over all possible configurations of neighboring beads along the protein chain. The resulting average dihedral potential of the residue is constant far enough from the cluster, but increases monotonically with decreasing distance below a threshold value. An overall potential around the cluster wherein a residue performs a chaotic motion is a combination of the average dihedral and pairwise potentials. As a function of distance from the cluster it has a double well shape. Residues in the inner well are considered as belonging to the cluster (folded part of the protein) while those in the outer well are treated as belonging to the unfolded (although compact) part of the protein. A double well shape of the potential around the cluster allows one to determine its emission and absorption rates by using a first passage time analysis and develop a self-consistent kinetic theory for the nucleation mechanism of protein folding. Numerical calculations for a protein of 2500 residues with the diffusion coefficient of residues in the native state ranging from 10^{-6} cm²/s to 10^{-8} cm²/s predict folding times in the range from several seconds to several hundreds of seconds.

*E-mail: idjikaev@eng.buffalo.edu

1 Introduction

Proteins play an overwhelmingly dominant role in life. If a specific job has to be done in a living organism, it is almost always a protein that does it. Life depends on thousands of different proteins whose structures are fashioned so that individual protein molecules combine, with exquisite precision, with other molecules. In order for a protein molecule to carry out a specific biological function, it has to adopt a well-defined three-dimensional structure.^{1,2} The formation of this structure (of a biologically active globular protein) constitutes the core of a so-called “protein folding problem”.³ Many thermodynamic and kinetic aspects of the process remain obscure and its mechanism elusive.^{4–8}

Experiment and simulation suggest that there exist multiple pathways for the protein folding.^{6–15} It is believed that initially a denatured protein very quickly transforms into a compact (but not native) configuration with a few, insignificant amount of tertiary contacts. The transition from such a compact configuration to the native one has been suggested to occur via two distinct mechanisms. One of them can be referred to as a “transition state mechanism” whereby the tertiary contacts of the native structure form as the protein passes through a sequence of intermediate states thus gradually achieving its unique spatial configuration.^{6–15} The protein in intermediate states has a native-like overall topology but is stabilized by incorrect hydrophobic contacts. These states correspond to misfolded forms of the native protein. The transition from these intermediate, misfolded states to the correctly folded, native structure is a slow process (because it involves a large-scale rearrangement of the molecule) occurring on a relatively large time scales.^{14,15} Alternatively, the transition from the compact “amorphous” configuration to the native state occurs immediately following the formation of some number of tertiary contacts.^{14,15} This mechanism is similar to nucleation, i.e., once a critical number of (native) tertiary contacts is established the native structure is formed without passing through any detectable intermediate states.¹⁴

So far most of the work on protein folding has been done by using either Monte Carlo (MC) or molecular dynamics (MD) simulations. A rigorous theoretical treatment of the problem by means of the statistical mechanics is hardly practicable because of the extreme complexity of the system, although some approximate treatments were already reported.^{16,17} A theoretical model for the nucleation mechanism of the process has so far remained underdeveloped.^{18,14,19} The model which existed so far is a thermodynamic one considering the formation of a cluster of protein residues and calculating its free energy change, much like the classical nucleation theory (CNT) does. The cluster is characterized by ν , the total number of residues, with the mole fraction of hydrophobic ones assumed to be known. As usual in CNT, the size of a critical cluster (nucleus) is provided by the location of the maximum of the free energy of formation as a function of ν . Such an approach necessarily involves the concept of surface tension for a cluster consisting of protein residues. (Clearly, this quantity is an intrinsically ill-defined physical quantity and can be considered only as an adjustable parameter; no direct experimental measurement thereof is possible.) After the formation of the nucleus (critical size cluster of residues), the protein quickly reaches its native state.

In what follows work I present a new, microscopic model for the nucleation mechanism of the protein folding. The new model is based on “molecular” interactions, both long-range (due to repulsion/attraction) and configurational (due bond and dihedral angles), in which protein residues are involved. Their parameters can be rigorously defined, and it should be possible (although not straightforward) to determine them theoretically, computationally, or experimentally. The ill-defined surface tension of a cluster of protein residues does not enter into the new model which

is thus more advanced than the CNT-based one. The crucial idea underlying the new model consists of averaging the dihedral potential in which a selected residue is involved over all the possible configurations of neighboring residues. The resulting average dihedral potential depends on the distance between residue and cluster. Its combination with the average long range potential (due to pairwise interactions of the selected residue with those in the cluster) gives rise to the overall potential which generates a pair of potential wells around the cluster with a barrier between them. Residues in the inner well are considered to belong to the cluster (part of the protein with correct tertiary contacts) while those in the outer well are treated as belonging to the mother phase (amorphous part of the protein with incorrect tertiary contacts). Transitions of residues from the inner well into the outer one and vice versa are considered as elementary emission and absorption events, respectively. The rates of emission and absorption of residues by the cluster are determined by using the first passage time analysis.^{20–25} Once these rates are found as functions of the cluster size, one can develop a self-consistent kinetic theory for the nucleation mechanism of folding of a protein. For example, the size of the critical cluster (nucleus) is then found as the one for which these rates are equal. The time necessary for the protein to fold can be evaluated as a sum of the times necessary for the appearance of the first nucleus and the time necessary for the nucleus to grow to the maximum size (of the folded protein in the native state).

The paper is structured as follows. In Section 2 we describe a random heteropolymer chain whereby a protein molecule is often modeled^{6,14} and outline a CNT-based model for the nucleation mechanism of protein folding, whereof a new, microscopic model is proposed in Section 3. The results of numerical calculations are presented in Section 4 and a brief discussion and conclusions are summarized in Section 5.

2 Heteropolymer chain as a protein model and a CNT based model for the nucleation mechanism of protein folding

2.1 A heteropolymer as a protein model

As a simple model of a protein in MD and MC simulations of protein folding dynamics, the polypeptide chain of a protein is considered^{6,14} as a heteropolymer consisting of N connected beads which can be thought of as representing the α -carbons of various amino acids. The heteropolymer may consist of hydrophobic (b), hydrophilic (l), or neutral (n). Two adjacent beads are connected by a covalent bond of fixed length η . This model (and its variants), augmented with appropriate interaction, bond, and dihedral potentials described below, was shown^{6,14,16,18} to be capable of capturing the essential characteristics of protein folding process even though it contains only some features of a real polypeptide chain. For example, this model ignores side groups although they are known to be crucial for intramolecular hydrogen bonding.¹ Besides, the presence of solvent (water) in a real physical system has been usually accounted for too simplistically, although the protein dynamics was reported to be more realistic in MD simulations where solvent molecules are explicitly present.²⁶ Despite these limitations, various modifications of heteropolymer models^{5,16,18,27–30} shed light on some important details of the folding of polypeptide chains, such as possible pathways for the protein transition from a denatured state to the native one.^{6,14}

The total energy of the heteropolymer (polypeptide chain) can contain the contributions of three different types. First, the contribution from repulsive/attractive forces between pairs of non-adjacent beads (these can be, e.g., of Lennard-Jones type or others). The next contribution

can arise from harmonic forces related with the oscillations of bond angles. Finally, there is a contribution from the dihedral angle potential due to the rotation around the peptide bonds. There are various ways to model these three types of energetic terms.^{6,14,27–29}

A pair interaction between two non-adjacent beads i and j at a distance r_{ij} away from each other can be taken, for example, as^{6,14}

$$\phi_{ij}(r_{ij}) = \begin{cases} 4\epsilon_b[(\eta/r_{ij})^{12} - (\eta/r_{ij})^6] & (i, j = b), \\ 4\epsilon_l[(\eta/r_{ij})^{12} + (\eta/r_{ij})^6] & (i = l, j = b, l), \\ 4\epsilon_n(\eta/r_{ij})^{12} & (i = n, j = b, l, n), \end{cases} \quad (1)$$

where η is the bond length (fixed) and ϵ_b , ϵ_l , and ϵ_n are the energy parameters.

The angle β between two successive bonds (in the heteropolymer) can be regarded to be subjected to a harmonic potential

$$\phi_\beta = \frac{k_\beta}{2}(\beta - \beta_0), \quad (2)$$

where the spring constant k_β is relatively large (in refs.6,14 it was taken $20\epsilon_b/(\text{rad})^2 = 105^\circ$ so that the deviation of the bond angles from the average value β_0 is very small. Hence all bond angles can be set to be equal to β_0 (as argued in refs.6,14, the bond angle forces play a minor role in the protein folding/unfolding).

The dihedral angle potential arises due to the rotation of three successive peptide bonds connecting four successive beads, and is related to the dihedral angle δ as

$$\phi_\delta = \epsilon'_\delta(1 + \cos \delta) + \epsilon''_\delta(1 + \cos 3\delta), \quad (3)$$

where ϵ'_δ and ϵ''_δ are independent energy parameters. This potential has three minima, one in the *trans* configuration at $\delta = 0$ and two others in the *gauche* configurations at $\delta = \pm \arccos \sqrt{(3\epsilon''_\delta - \epsilon'_\delta)/12\epsilon''_\delta}$ (the former one is lower than the latter two).

The above structure of potential functions for a heteropolymer was suggested by Honeycutt and Thirumalai,⁶ while Bryngelson and Wolynes^{16,18} used a random energy model and Skolnik and co-workers^{27–29} developed discrete analogs (for a diamond lattice) of eqs.(1) and (3) augmented with a “cooperativity potential” as a crucial element of the model. It was shown^{6,14} by MD simulations (employing low friction Langevin dynamics) that a proper balance between the above three contributions to the total energy of the heteropolymer ensures that the heteropolymer folds into a well defined β -barrel structure. The balancing between these terms is performed by adjusting the energy parameters ϵ_b , ϵ_l , ϵ_n , ϵ'_δ , ϵ''_δ for each type of beads. It was also found^{6,14} that the balance between the dihedral angle potential, which tends to stretch the molecule into a state with all bonds in a *trans* configuration, and the attractive hydrophobic potential is crucial to induce folding into a β -barrel like structure upon cooling. Excessively dominant attractive forces make the heteropolymer fold into a globule-like structure, while an overwhelming dihedral angle potential makes the chain remain in an unfolded (elongated) state (even at low temperatures) with bonds mainly in the *trans* configuration.

A possibility that the nucleation-like mechanism can constitute the most viable pathway for the protein folding was first suggested by Guo and Thirumalai¹⁴ (although Bringelson and Wolynes¹⁸ also drew the analogy between the results presented therein and the thermodynamics of cluster formation in the framework of CNT). The formalism of the nucleation mechanism for the protein folding is invoked to evaluate the size of the critical cluster (nucleus) of native protein residues (whereof the formation leads to a quick transition of the whole protein into its native state).

Denoting the total number of residues in the protein by N_0 , let us consider a formation of a cluster having a correct tertiary structure in an unfolded protein. The free energy of formation of such a cluster of ν native residues (i.e., residues which are in the same state as they are in the native protein) can be written (in the framework of CNT) as

$$W = -\nu\Delta\mu + \sigma 4\pi\lambda^2\nu^{2/3}, \quad (4)$$

where $\delta\mu \equiv \mu_d - \mu_n$ is the difference between the free energy per residue in the denatured and native states, respectively (marked with the subscripts “d” and “n”), σ is the “surface” tension (energy) of the boundary between the cluster (having a native structure) and the unfolded part of the protein, $\lambda = (3v/4\pi)^{1/3}$, and v is a volume per protein residue in its native state.

In ref.14 it was argued that the initial stage of the protein folding is driven by a hydrophobic attractive forces so that the volume term (i.e., the first one) in eq.(4) was determined by the number of hydrophobic contacts in the cluster and hence could be specified as $-(1/2)\epsilon_b\chi\nu(\chi\nu-1)$, where χ is the mole fraction of hydrophobic residues in the cluster (assumed the same as in the whole protein). As a result the number of residues in the critical cluster was given as $\nu_c = (8\pi\sigma\lambda^2/3\chi^2\epsilon_b)^{(3/4)}$ which for typical values of λ, σ , and ϵ_b was estimated¹⁴ to be of the order of 10. In ref.16, $\Delta\mu$ in the volume term of eq.(4) was evaluated to be of the order of $0.1k_BT$ (k_B is the Boltzmann constant, and T is the temperature). The “surface” tension was argued to arise because the amino acid residues located at the cluster surface interact stronger with the cluster interior than with the unfolded part of the protein. Since the interaction energies in protein folding are of the order of k_BT , the surface tension σ multiplied by $4\pi\lambda^2$ was estimated to be of the same order and the number of residues in the critical cluster was evaluated¹⁸ to be of the order of 100 (for $N_0 = 150$). Both estimates corroborate the idea that the nucleation mechanism can constitute a viable pathway for the protein folding.^{31–35}

3 Kinetics of nucleation during protein folding

The CNT-based model for the nucleation mechanism of protein folding is limited to its thermodynamics, namely to the free energy of formation of the cluster of native residues. For a system in the thermodynamic limit (both the number of molecules $N \rightarrow \infty$ and the volume $V \rightarrow \infty$), the validity of expression (4) for the free energy of cluster formation in various [i.e., canonical (NVT), grand canonical (μ VT), and Gibbs (NPT)] ensembles was well established.^{36,37} If nucleation occurs in a finite size system, there appear additional terms on the RHS of eq.(4) which depend not only on the size of the system but also on the nature of the ensemble. However, a folding protein (mostly containing much less than a couple of thousands of amino acids) can hardly be considered to satisfy the thermodynamic limit. Furthermore, the cluster formation during protein folding occurs under conditions which cannot be identified with either of commonly used thermodynamic ensembles. Besides, the CNT based model (described above) has inherited a complicated problem of CNT related to the surface tension of the cluster. It was argued that the concept of surface tension may not be adequate for too small clusters (such as those of interest in nucleation),^{38,39} not to mention the assumption (of CNT) that it is equal to the surface tension of a planar interface. Although CNT produces reasonable agreement with experiment on unary nucleation, its application to multicomponent nucleation leads to several inconsistencies and large discrepancies with experimental data^{40–45} which are blamed on the inadequate use of the concept of surface tension. In the case of protein folding this problem is even more complicated because σ in eqs.(4) is

an ill-defined quantity which is experimentally impossible to determine due to the non-existence of bulk “folded protein” and “unfolded protein” as real physical phases, not to mention a flat interface between them.

In order to avoid the use of macroscopic thermodynamics in the kinetic theory of unary nucleation, an alternative approach was proposed^{20–22} on the basis of the mean first passage time analysis. Unlike CNT, that theory^{20–22} is built upon molecular interactions and does not make use of the free energy of formation of tiny clusters involved in nucleation. Instead, the theory^{20–22} exploits the fact that one can derive and solve the kinetic equation of nucleation (hence find the nucleation rate) if the emission and absorption rates of a cluster are known as functions of its size. For the rate of absorption of molecules by the cluster, the new approach uses (as CNT does) a standard gas-kinetic expression,⁴⁶ but the rate of emission of molecules by the cluster is determined via a mean first passage time analysis. This time is calculated by solving a single-molecule master equation for the probability distribution function of a surface layer molecule moving in a potential well around the cluster. The master equation is a Fokker-Planck equation in the phase space which can be reduced to the Smoluchowski equation owing to the hierarchy of characteristic time scales in the evolution of the single-molecule distribution function with respect to coordinates and momenta.^{20–22} Recently, a further development of that kinetic theory was proposed by combining it with the density functional theory (DFT)^{23,24} and extending it to binary²⁴ and heterogeneous²⁵ systems.

Note that although the emission rate of the cluster in refs.20-25 was found by using a first passage time analysis, for the absorption rate there was used an expression derived in the framework of the gas-kinetic theory of gases⁴⁶ which assumes a Maxwellian distribution of velocities of mother phase molecules. This assumption being unquestionably valid for vapor-to-liquid nucleation in dilute (if not ideal) gases, becomes increasingly inaccurate as the density of the mother phase increases and molecular interactions therein become non-negligible. Clearly, this assumption (hence the absorption rate based thereupon) is inadequate in considering the cluster formation during the protein folding. Indeed, the amino acid residues of the protein are all successively linked by bonds of virtually fixed length each and fixed angle between each pair.

In this section we will present a new, kinetic model for the nucleation mechanism of protein folding based on the first passage analysis which will be used for determining not only the rate of emission (of native residues from the cluster) but also the rate of absorption (of non-native residues by the cluster). The general formalism of our model is a mean first passage time analysis, but a crucial modification (compared to refs.20-25) must be introduced thereto in order to make it applicable to nucleation in a protein. This modification concerns the potential well generated around the cluster as a result of all its interactions with a residue which moves around the cluster while being a part of the protein backbone (a bead in a heteropolymer).

3.1 Potential well around a cluster within a protein

A heteropolymer chain as a protein model, originally proposed in refs.6,14 and described above, consists of three types of beads - neutral, hydrophobic, and hydrophilic. The neutral beads play an important role in that model. Their interaction with each other is purely repulsive and the dihedral angle forces are assumed to be weaker for the bonds involving them so that the bend formation is enhanced in regions where they are present. In real proteins this kind of residues can be thought to ensure the formation of loops and turns. MD simulations^{6,14} show that such a heteropolymer acquires a β -barrel shape in the lowest energy structure, with neutral residues

appearing mostly in bend regions. This work is not aimed at obtaining a β -barrel structure of the folded protein, so neutral beads will be removed from the model. Clearly, this will require to rebalance ϵ 's in eqs.(1),(3) in order to facilitate the formation of loops and turns in a heteropolymer chain.

Thus, the two-component heteropolymer chain as a model for a protein consists of only hydrophobic and hydrophilic beads without neutral ones with the pair interaction, bond angle, and dihedral angle potentials given by eqs.(1)-(3). With this assumption, the formation of a cluster consisting of native residues during the protein folding can be regarded as binary nucleation. We shall therefore present a model for the nucleation mechanism of protein folding in terms of binary nucleation by using a first passage time analysis^{20–25} with a crucial modification concerning the potential well around the cluster.

Consider a binary cluster of spherical shape (with sharp boundaries and radius R) immersed in a binary fluid mixture.²⁴ A molecule of component i ($i = b, l$) located in the surface layer of the cluster was considered to perform thermal chaotic motion in a spherically symmetric potential well $\phi_i(r)$ resulting from the pair interactions of this molecule with those in the cluster. Assuming pairwise additivity of the intermolecular interactions, $\phi_i(r)$ is provided by

$$\phi_i(r) = \sum_j \int_V d\mathbf{r}' \rho_j(r') \phi_{ij}(|\mathbf{r}' - \mathbf{r}|), \quad (5)$$

Here \mathbf{r} is the coordinate of the surface molecule i , $\rho_j(r)$ ($j = 1, 2$) is the number density of molecules of component j at point \mathbf{r}' (spherical symmetry is assumed, the cluster center chosen as the origin of the coordinate system), and $\phi_{ij}(|\mathbf{r}' - \mathbf{r}|)$ is the interaction potential between two molecules of components i and j at points \mathbf{r} and \mathbf{r}' , respectively. The integration in eq.(5) goes over the whole volume of the system, but the vapor phase contribution can be assumed to be small and accounted for by a particular choice of the ϵ_b and ϵ_l .

For nucleation in proteins the potential $\psi_i(r)$ for a residue of type i around the cluster is determined not only by the potential $\phi_i(r)$, but also by two other contributions, $\phi_\beta(r)$ and $\bar{\phi}_\delta(r)$, due to the bond angle and dihedral angle potentials, respectively:

$$\psi_i(r) = \phi_i(r) + \phi_\beta(r) + \bar{\phi}_\delta(r).$$

Without affecting the generality of the model, one can significantly simplify the algebra and eventual numerical calculations by assuming that all bond angles are fixed and equal to $\beta_0 = 105^\circ$. Under this assumption the contribution to the potential energy of the protein arising from the bond angle potential is constant and does not depend on the distance r between the selected bead and the center of the cluster. Therefore, the term $\phi_\beta(r)$ on the RHS of eq.(6) can be disregarded (or, equivalently, be chosen as a reference level for the potential energy), i.e.,

$$\psi_i(r) = \phi_i(r) + \bar{\phi}_\delta(r). \quad (6)$$

The term $\phi'_\delta(r) \equiv \phi'_\delta(r, \mathbf{r}_2, \mathbf{r}_3, \mathbf{r}_4, \mathbf{r}_5, \mathbf{r}_6, \mathbf{r}_7)$ in $\psi_i(r)$ is due to the dihedral angle potential of the whole protein. Consider bead 1 (of type b or l) at a distance r from the center of the cluster (see Figure 1). The total dihedral angle potential of the whole protein chain for a given configuration of beads 2,3,...,N can be written in the form

$$\phi'_\delta(r) = \phi_\delta(\delta_{421}^{642}(r)) + \phi_\delta(\delta_{213}^{421}(r)) + \phi_\delta(\delta_{135}^{213}(r)) + \phi_\delta(\delta_{357}^{135}(r)). \quad (7)$$

where δ_{jkl}^{ijk} is a dihedral angle between two planes, one of which is determined by beads i, j, k and the other by beads j, k, l . On the RHS of the above equation, an independent of r term is omitted which represents the contributions from the dihedral angles involving beads $8, 9, \dots, N$ (hence $\phi'_\delta(r)$ does not depend on coordinates of beads $8, \dots, N_0$). It can be regarded as affecting only the reference level for $\psi_i(r)$.

Consider bead 1 at a given distance from the cluster r . Various configurations of beads $2, 3, \dots, N$ (subject to the fixed bond length and bond angle constraints as well as to the constraint of excluded cluster volume) lead to various sets of dihedral angles. However, variations in the location of beads $8, 9, \dots, N$ lead to variations in the dihedral potential which are independent of r . Thus, the dihedral term $\bar{\phi}_\delta(r)$ (less an independent of r term omitted hereafter) on the RHS of eq.(7) can be obtained by averaging eq.(8) with the probability distribution function $p(\mathbf{r}, \mathbf{r}_2, \mathbf{r}_3, \mathbf{r}_4, \mathbf{r}_5, \mathbf{r}_6, \mathbf{r}_7)$ for configurations of beads 2 to 7 with a fixed location of bead 1 and assigning the result to the latter:

$$\bar{\phi}_\delta(r) = \int_{\Omega_{18}} d\mathbf{r}_2 d\mathbf{r}_3 d\mathbf{r}_4 d\mathbf{r}_5 d\mathbf{r}_6 d\mathbf{r}_7 \phi'_\delta(r) p(\mathbf{r}, \mathbf{r}_2, \mathbf{r}_3, \mathbf{r}_4, \mathbf{r}_5, \mathbf{r}_6, \mathbf{r}_7) \quad (8)$$

where \mathbf{r}_i ($i = 2, \dots, 7$) is the radius-vector of bead i and Ω_{18} is the integration region in an 18-dimensional space.

It is convenient to choose a Cartesian system of coordinates with the origin in the cluster center in such a way that the coordinates of bead 1 are $x_1 = 0, y_1 = 0, z_1 = r$ (see Figure 1). The Cartesian coordinates of other beads will be denoted by x_i, y_i, z_i ($i = 2, \dots, 7$). The Cartesian coordinates of bead 2 are related to its spherical ones r_2, Θ_2, φ_2 by

$$x_2 = r_2 \sin \Theta_2 \cos \varphi, \quad y_2 = r_2 \sin \Theta_2 \sin \varphi, \quad z_2 = r_2 \cos \Theta_2. \quad (9)$$

At a given r (the location of bead 1 is fixed), the polar angle Θ of bead 2 is uniquely determined by r_2 due to the constant bond length constraint:

$$\tilde{\Theta}_2 = \Theta_2(r, r_2) = \arccos[(r^2 + r_2^2 - \eta^2)/(2r_2r)] \quad (0 \leq \tilde{\Theta}_2 \leq \pi), \quad (10)$$

whereas the azimuthal angle $0 \leq \varphi_2 \leq 2\pi$. The distance r_2 varies in the range

$$r_{2\min} \leq r_2 \leq r + \eta, \quad (11)$$

where $r_{2\min} = \max(R, r - \eta)$. Thus the integration with respect to \mathbf{r}_2 in eqs.(8) reduces to integration with respect to φ_2 and r_2 with fixed $\Theta_2 = \tilde{\Theta}_2$.

For given locations of beads 1 and 2, the possible locations of beads 3 and 4 lie on circles of radius $r_0 = \eta \sin \beta_0$ with their location and orientation completely determined by the coordinates of beads 1 and 2. This is due to the constraints that all bond angles are equal to β_0 and all bond lengths are equal to η . Due to the same constraints, if the locations of beads 2 and 4 are given, the possible locations of bead 6 lie on a circle of radius r_0 , whereof the location and orientation are completely determined by the coordinates of beads 2 and 4. Further, for the given locations of beads 1 and 3, the possible locations of bead 5 lie on a circle of radius r_0 with the position and orientation completely determined by the coordinates of beads 1 and 3. Finally, for the given locations of beads 3 and 5, the possible locations of bead 7 are on a circle of radius r_0 , with the location and orientation completely determined by the coordinates of beads 3 and 5.

Let us consider bead s with unknown coordinates and two other beads, c and n (closest to and next to the closest to bead s) with known coordinates x_c, y_c, z_c and x_n, y_n, z_n . For example,

if $s = 7$, then $c = 5, n = 3$; if $s = 4$, then $c = 2, n = 1$. Bead s lies on a circle of radius r_0 with the coordinates of the center

$$x_0 \equiv x_0(x_n, y_n, z_n, x_c, y_c, z_c) = x_n + (x_c - x_n) \frac{\eta(1 + |\cos \Theta_0|)}{\sqrt{(x_c - x_n)^2 + (y_c - y_n)^2 + (z_c - z_n)^2}}, \quad (12)$$

$$y_0 \equiv y_0(x_n, y_n, z_n, x_c, y_c, z_c) = y_n + (y_c - y_n) \frac{\eta(1 + |\cos \Theta_0|)}{\sqrt{(x_c - x_n)^2 + (y_c - y_n)^2 + (z_c - z_n)^2}}, \quad (13)$$

$$z_0 \equiv z_0(x_n, y_n, z_n, x_c, y_c, z_c) = z_n + (z_c - z_n) \frac{\eta(1 + |\cos \Theta_0|)}{\sqrt{(x_c - x_n)^2 + (y_c - y_n)^2 + (z_c - z_n)^2}}. \quad (14)$$

The coordinate x_s of bead s can change in the range

$$x_c - x_b \leq x_s \leq x_c + x_b \quad (s = 3, \dots, 7), \quad (15)$$

where

$$x_b \equiv x_b(x_n, y_n, z_n, x_c, y_c, z_c) = \eta \sin \Theta_0 \sqrt{\frac{((y_c - y_0)^2 + (z_c - z_0)^2)}{(x_c - x_n)^2 + (y_c - y_n)^2 + (z_c - z_n)^2}}. \quad (16)$$

For a given x_s , the coordinate y_s of bead s can have only one of two values,

$$\begin{aligned} y_s^\pm &\equiv y_s^\pm(x_s, x_n, y_n, z_n, x_c, y_c, z_c) = y_0 + \frac{(-(x_c - x_0)(y_c - y_0)(x_s - x_0)}{(y_c - y_0)^2 + (z_c - z_0)^2} \pm \\ &\quad \frac{|z_c - z_0| \sqrt{[(y_c - y_0)^2 + (z_c - z_0)^2] \eta^2 \sin^2 \beta_0 - [(x_c - x_n)^2 + (y_c - y_n)^2 + (z_c - z_n)^2] (x_s - x_0)^2}}{(y_c - y_0)^2 + (z_c - z_0)^2}, \end{aligned} \quad (17)$$

For given x_s and y_s , the coordinate z_s of bead s can have only a single value

$$z_s^\pm \equiv z_s(x_s, y_s^\pm, x_n, y_n, z_n, x_c, y_c, z_c) = z_0 - \frac{(x_c - x_0)(x_s - x_0) + (y_c - y_0)(y_s - y_0)}{z_c - z_0}. \quad (18)$$

Thus, the probability distribution function $p(\mathbf{r}, \mathbf{r}_2, \mathbf{r}_3, \mathbf{r}_4, \mathbf{r}_5, \mathbf{r}_6, \mathbf{r}_7)$ acquires the form

$$\begin{aligned} p(\mathbf{r}, \mathbf{r}_2, \mathbf{r}_3, \mathbf{r}_4, \mathbf{r}_5, \mathbf{r}_6, \mathbf{r}_7) &= f^{-1} \delta(\Theta_2 - \tilde{\Theta}_2) \Pi_{i=3}^7 [\delta(y_i - y_i^-) + \delta(y_i - y_i^+)] \delta(z_i - \tilde{z}_i) \times \\ &\quad \exp[-\phi'_\delta(r, (\mathbf{r}, \mathbf{r}_2, \mathbf{r}_3, \mathbf{r}_4, \mathbf{r}_5, \mathbf{r}_6, \mathbf{r}_7))], \end{aligned} \quad (19)$$

where f is a normalization constant determined by the condition

$$\int_{\Omega_{18}} d\mathbf{r}_2 d\mathbf{r}_3 d\mathbf{r}_4 d\mathbf{r}_5 d\mathbf{r}_6 d\mathbf{r}_7 p(\mathbf{r}, \mathbf{r}_2, \mathbf{r}_3, \mathbf{r}_4, \mathbf{r}_5, \mathbf{r}_6, \mathbf{r}_7) = 1. \quad (20)$$

Substituting eq.(19) into eq.(8) reduces an 18-fold integral to a 7-fold one:

$$\begin{aligned} \bar{\phi}_\delta(r) &= f^{-1} \sum_{i,j,k,m,n=+,-} \int_0^{2\pi} d\varphi_2 \int_{L_2} dr_2 \int_{L_3^i} dx_3 \int_{L_4^j} dx_4 \int_{L_5^k} dx_5 \int_{L_6^m} dx_6 \int_{L_7^n} dx_7 \times \\ &\quad r_2^2 \sin \Theta_2(r, r_2) \tilde{\phi}_{ijkmn}(\varphi_2, r_2, x_3, \dots, x_7) \exp[-\tilde{\phi}_{ijkmn}(\varphi_2, r_2, x_3, \dots, x_7)/k_B T], \end{aligned} \quad (21)$$

$$\begin{aligned}
f = & \sum_{i,j,k,m,n=+,-} \int_0^{2\pi} d\varphi_2 \int_{L_2} dr_2 \int_{L_3^i} dx_3 \int_{L_4^j} dx_4 \int_{L_5^k} dx_5 \int_{L_6^m} dx_6 \int_{L_7^n} dx_7 \times \\
& r_2^2 \sin \Theta_2(r, r_2) \exp[-\tilde{\phi}_{ijkmn}(\varphi_2, r_2, x_3, \dots, x_7)/k_B T].
\end{aligned} \tag{22}$$

In these equations each of the summation indices takes on two values, + and -, so that there are 5^2 terms in the sum differing by the integrand as well as by the integration ranges (except for L_2 which is independent of i, j, k, m, n).

The double inequalities (11) and (15) and eqs.(16)-(18) completely determine the integration ranges (subject to the additionl constraint $x_s^2 + y_s^2 + z_s^2 > R^2$ ($s = 2, \dots, 7$) of excluded cluster volume) in eqs.(21) and (22). In order to transform the function $\phi'_\delta(r) \equiv \phi'_\delta(r, \mathbf{r}_2, \mathbf{r}_3, \mathbf{r}_4, \mathbf{r}_5, \mathbf{r}_6, \mathbf{r}_7)$ into the function $\tilde{\phi}_{ijkmn}(r, \varphi_2, r_2, x_3, \dots, x_7)$, the variables y_s ($s = 3, \dots, 7$) and z_s ($s = 3, \dots, 7$) in the former must be replaced by y_s^\pm and z_s^\pm in all the possible combinations each of which gives rise to a term in the sums in eqs.(21) and (22) (note that $z_s^+ = z_s(x_s, y_s^+, \dots)$ and $z_s^- = z_s(x_s, y_s^-, \dots)$). The polar angle of bead 2 must be replaced by $\tilde{\Theta}_2 = \Theta_2(r, r_2)$.

For example, consider the term with $i = +, j = -, k = +, m = +, n = -$ in the sum in eqs.(21),(22). The corresponding integrand $\tilde{\phi}_{+-+-+}(\varphi_2, r_2, x_3, \dots, x_7)$ is obtained from

$\phi_\delta(r, \mathbf{r}_2, \mathbf{r}_3, \mathbf{r}_4, \mathbf{r}_5, \mathbf{r}_6, \mathbf{r}_7)$ as follows:

y_3 must be replaced by $y_3^+ \equiv y_3^+(x_3, x_2, y_2, z_2, x_1, y_1, z_1)$ and z_3 by $z_3^+ \equiv z_3(x_3, y_3^+, x_2, y_2, z_2, x_1, y_1, z_1)$, y_4 must be replaced by $y_4^- \equiv y_4^-(x_4, x_1, y_1, z_1, x_2, y_2, z_2)$ and z_4 by $z_4^- \equiv z_4(x_4, y_4^-, x_1, y_1, z_1, x_2, y_2, z_2)$, y_5 must be replaced by $y_5^+ \equiv y_5^+(x_5, x_1, y_1, z_1, x_3, y_3, z_3)$ and z_5 by $z_5^+ \equiv z_5(x_5, y_5^+, x_1, y_1, z_1, x_3, y_3, z_3)$, y_6 must be replaced by $y_6^+ \equiv y_6^+(x_6, x_2, y_2, z_2, x_4, y_4, z_4)$ and z_6 by $z_6^+ \equiv z_6(x_6, y_6^+, x_2, y_2, z_2, x_4, y_4, z_4)$, y_7 must be replaced by $y_7^- \equiv y_7^-(x_7, x_3, y_3, z_3, x_5, y_5, z_5)$ and z_7 by $z_7^- \equiv z_7(x_7, y_7^-, x_3, y_3, z_3, x_5, y_5, z_5)$,

Figure 2 presents $\phi_\delta(r)$, the contribution from the average dihedral potential to the total potential around the cluster, provided by eqs.(21),(22). It has quite a remarkable behavior. Starting with its maximum value at the cluster surface, it monotonically decreases with increasing r until it becomes constant for some $r \geq \tilde{r}$ (see section 4). This behaviour can be accounted for by the entropic effect on the average dihedral potential assigned to a selected bead. Actually, the closer the selected bead (1) is to the cluster surface (for $r < \tilde{r}$), the more restricted is the configurational space available for the neighboring beads (2 through 7). This decreases the entropy of the heteropolymer chain compared to the case where bead is far enough away from the cluster which, in turn transpires as an increase in the average dihedral potential $\phi_\delta(r)$, assigned to bead 1, with decreasing r . With some degree of liberty, $\phi_\delta(r)$ can be interpreted as a constrained (with bead 1 fixed) free energy of the heteropolymer chain 1 through 7.

3.2 Determination of the emission and absorption rates

Figure 3 presents typical shapes of the constituents $\phi_i(r)$ and $\phi_\delta(r)$ of the potential well as functions of the distance from the cluster center, as well as the overall potential well $\psi_i(r)$ itself (for details of numerical calculations see section 4). The contribution $\phi_i(r)$, arising from the pairwise interactions, has a familiar form^{20–25} reminiscent of the underlying Lennard-Jones potential. Its combination with the contribution $\phi_\delta(r)$ from the average dihedral potential results in the overall potential $\psi_i(r)$ which has a double well shape: the inner well is separated by the potential barrier from the outer well. This shape of $\psi_i(r)$ is of crucial importance to our model for the nucleation mechanism of protein folding because it makes it possible to use a mean first passage time analysis for the determination of the rate of absorption of beads by the cluster

Developing our model in the spirit of the mean first passage time analysis,^{20–25} a bead (residue)

is considered as belonging to the cluster as long as it remains in the inner potential well (hereinafter referred to as “i.p.w.”), and as dissociated from the cluster when it passes over the barrier between the i.p.w. and the outer potential well (hereinafter referred to as “o.p.w.”). The rate of emission, W^- , is determined by the mean time necessary for the passage of the bead from the i.p.w. over the barrier into the o.p.w. Likewise, a bead is considered as belonging to the unfolded part of the heteropolymer (protein) as long as it remains in the o.p.w., and as absorbed by the cluster when it passes over the barrier between the o.p.w. and the i.p.w.. The rate of emission, W^+ , is determined by the mean time necessary for the passage of the bead from the o.p.w. over the barrier into the i.p.w.

The mean first passage time of a bead escaping from some potential well is calculated on the basis of a kinetic equation governing the chaotic motion of the bead in that potential well. The chaotic motion of the bead is assumed to be governed by the Fokker-Planck equation for the single-particle distribution function with respect to its coordinates and momenta, i.e., in the phase space.^{47–49} Prior to the passage event, the evolution of a bead in both the i.p.w. and o.p.w. occurs in a dense enough medium (cluster folded residues or unfolded but compact part of the protein), where the relaxation time for its velocity distribution function is extremely short and negligible compared to the characteristic time scale of the passage process. Under favorable conditions, the Fokker-Planck equation reduces to the Smoluchowski equation, which involves diffusion in an external field.^{48,49} Solving that equation, one can obtain²⁴ the following expressions for W^- and W^+ , the emission and absorption rates, respectively:

$$W^- = n_{\text{iw}} D_{\text{iw}} \omega_{\text{iw}}, \quad W^+ = n_{\text{ow}} D_{\text{ow}} \omega_{\text{ow}}. \quad (23)$$

Here the subscripts “iw” and “ow” mark the quantities for the inner and outer potential wells, respectively; n is the number of beads in the well, D is the diffusion coefficient of the bead, and ω_{iw} and ω_{ow} are defined as

$$\omega_{\text{iw}} \equiv 1/D_{\text{iw}} \bar{\tau}_{\text{iw}}, \quad \omega_{\text{ow}} \equiv 1/D_{\text{ow}} \bar{\tau}_{\text{ow}}, \quad (24)$$

where $\bar{\tau}_{\text{iw}}$ and $\bar{\tau}_{\text{ow}}$ are the mean first passage times for a bead in the i.p.w. to cross over the barrier into the o.p.w. and vice-versa, respectively. Note that in the original work^{20–22} on the mean first passage time analysis in the nucleation theory and its recent development^{23–25} this method was used only for determining W^- but not W^+ . In the present model, the double well character of the overall potential $\psi(r)$ around the cluster allows one to apply the first passage time analysis also to determining W^+ .

Clearly, the quantities W^- , W^+ , ω_{iw} , ω_{ow} , $\bar{\tau}_{\text{iw}}$, $\bar{\tau}_{\text{ow}}$ are the functions of the cluster size and composition (for the explicit form see ref.24). However, since the overall composition of the protein (heteropolymer) is fixed, one can assume that the cluster which forms during its folding has a constant composition equal to the overall protein composition which leads to a unary nucleation theory. (Strictly speaking, one can develop a theoretical model for the nucleation mechanism of protein folding without this assumption which would lead to a binary nucleation theory, but this would drastically complicate the problem computationally.) Under this assumptions the aforementioned quantities are functions of only the size of the cluster (say, its radius R or the total number of beads ν therein).

3.3 The equilibrium distribution and steady-state nucleation rate

In terms of nucleation, during the protein folding clusters of various sizes may emerge and exist simultaneously with different probabilities. Let us denote the distribution of clusters with respect

to the number of beads in a cluster at time t by $g(\nu, t)$. Once the emission and absorption rates $W^- = W^-(\nu)$ and $W^+ = W^+(\nu)$ are known as functions of the cluster size, one can find the equilibrium distribution of clusters $g_e(\nu, t)$ and solve the kinetic equation of nucleation to find the steady-state nucleation rate.

Actually, according to the principle of detailed balance, $W^+(\nu - 1)g_e(\nu - 1) = W^-(\nu)g_e(\nu)$, which can be rewritten as

$$\frac{g_e(\nu)}{g_e(\nu - 1)} = \frac{W^+(\nu - 1)}{W^-(\nu)}. \quad (25)$$

By applying eq.(25) to $(\nu - i)$ with $i = 2, 3, \dots, \nu - 1$, multiplying the RHSs and LHSs of all equalities, one obtains

$$\frac{g_e(\nu)}{g_e(1)} = \prod_{i=1}^{\nu-1} \frac{W^+(\nu - i)}{W^-(\nu - i + 1)}. \quad (26)$$

The equilibrium distribution of clusters $\nu = 1$ is just the number density of residues in a compact (but unfolded) protein, i.e., $g_e(1) = \rho_u$, so that equation (18) can be rewritten as

$$g_e(\nu) = \rho_u \frac{W^+(1)}{W^+(\nu)} \prod_{i=1}^{\nu-1} \frac{W^+(\nu - i + 1)}{W^-(\nu - i + 1)}. \quad (27)$$

Let us introduce the function $G(\nu) = -k_B T \ln[g_e(\nu)/\rho_u]$. Clearly, $G(\nu)$ in the present theory plays a role similar to the free energy of cluster formation in CNT^{50–52}. Under favorable conditions, $G(\nu)$ first increases with increasing ν , attains its maximum at some $\nu = \nu_c$, and then decreases. In CNT, $G(\nu)$ has also a minimum following the maximum but only for an NVT ensemble where the growth of the cluster (i.e., increase of ν) leads to the decrease in the metastability of the mother phase. Since the folding protein cannot be considered as an NVT ensemble, we will not consider this case. The essence of our model, as an alternative to the CA-based theory, consists of constructing the equilibrium distribution of clusters, $g_e(\nu)$ (and the function $G(\nu)$) without employing the classical thermodynamics.

The kinetic equation of nucleation in the vicinity of the critical point can be written as^{50–52}

$$\frac{\partial g(\nu, t)}{\partial t} = W_c^+ \frac{\partial}{\partial \nu} \left[\frac{\partial}{\partial \nu} + \frac{\partial G}{\partial \nu} \right] g(\nu, t). \quad (28)$$

(subscript “c” marks quantities at the critical point) and the function $G(\nu)$ can be accurately represented by its bilinear form. The steady-state solution of the kinetic equation (20) in the vicinity of ν_c subject to the conventional boundary conditions

$$\frac{g(\nu, t)}{g_e(\nu)} \rightarrow 1 \quad (\nu \rightarrow 0), \quad \frac{g(\nu, t)}{g_e(\nu)} \rightarrow 0 \quad (\nu \rightarrow \infty), \quad (29)$$

where $g_e(\nu)$ is the equilibrium distribution, provides the steady-state nucleation rate^{50–52} which can be presented in the form

$$J_s = \frac{W_c^+}{\sqrt{\pi} \Delta \nu_c} \rho_u e^{-G_c/k_B T}, \quad (30)$$

where

$$\Delta \nu_c = \left| \frac{\partial^2 G}{\partial \nu^2} \right|_c^{-1/2}. \quad (31)$$

3.4 Evaluation of the protein folding time

Knowing the emission and absorption rates as functions of ν as well as the nucleation rate J_s , one can estimate the time t_f necessary for the protein to fold via nucleation. To do so we will regard the protein folding (via nucleation) as a two stage process. At the first stage, a critical cluster of native residues form (nucleation proper). At this stage, i.e., for $\nu < \nu_c$, the emission rate W^- is larger than W^+ , but the cluster does attain the critical size by means of fluctuations. At the second stage the nucleus grows via regular absorption of native residues dominating their emission, $W^- < W^+$ for $\nu > \nu_c$. Thus, the folding time can be represented as

$$t_f \simeq t_n + t_g, \quad (32)$$

where t_n is the time necessary for one critical cluster to nucleate within a compact (but still unfolded) protein and t_g is time necessary for the nucleus to grow up to the maximum size, i.e., attain the size of a folded protein.

The time t_n of the first nucleation event can be estimated as

$$t_n \simeq 1/J_s V_0, \quad (33)$$

where V_0 is the volume of the unfolded protein in a compact state. The growth time t_g can be found by solving the differential equation

$$\frac{d\nu}{dt} = W^+(\nu) - W^-(\nu) \quad (34)$$

subject to the initial condition $\nu = \nu_c$ at $t = 0$ and the condition $\nu = N_0$ at $t = t_n$. The solution of eq.(34) is given by the integral

$$t_n \simeq \int_{\nu_c}^{N_0} \frac{d\nu}{W^+(\nu) - W^-(\nu)}. \quad (35)$$

4 Numerical evaluations

In this section we will present some numerical results of the application of our model to the folding of a model protein, namely, a heteropolymer consisting of total 2500 hydrophobic and hydrophilic residues, with the mole fraction of hydrophobic residues $\chi_0 = 0.75$. The interactions between a pair of non-linked beads were modeled via the Lennard-Jones (LJ) type potentials (1), while the potential due to the dihedral angle δ was modeled according to eq.(3). The presence of water molecules was not taken into account explicitly but was assumed to be implemented into the model via the potential parameter.

All numerical calculations were carried out for the following values of the interaction parameters:

$$\eta_1 = 5.39 \times 10^{-8} \text{ cm}, \quad \epsilon_l = (2/700)\epsilon_b, \quad \epsilon'_\delta = \epsilon''_\delta = 0.3\epsilon_b, \quad \epsilon_b/kT = 1.$$

A typical density of the folded protein was evaluated according to data in refs.53,54 and was set to $\rho_f \eta^3 = 1.05$, while a typical density of the unfolded protein in the compact configuration was set to be $\rho_u = 0.25\rho_f$ (note that similar values for ρ_f and ρ_d are suggested in ref.18). Taking into account the results in ref.55, the diffusion coefficients in the i.p.w. and the o.p.w. were assumed to be related as $D_{\text{iw}}\rho_f = D_{\text{ow}}\rho_u$. Because of the lack of reliable data on the diffusion

coefficient of a residue in a protein chain, D_{iw} was assumed to vary between 10^{-6} cm²/s and 10^{-8} cm²/s.

Figure 2 shows the average dihedral potential (assigned to a selected bead) $\bar{\phi}^\delta(r)$ as a function of r for three clusters of sizes (a) $R = 3\eta$, (b) $R = 6\eta$, and (c) $R = 9\eta$. The points represent the actual numerical results obtained by using 1×10^6 to 2×10^6 point Monte Carlo integration in calculating 7-fold integrals in eqs.(11),(12). The vertical dashed lines correspond to r' (see above) such that $\bar{\phi}^\delta(r)$ is expected to be constant for $r > r'$. The solid lines are analytic fits by an expression $a + b \exp[-c(r - d)^2]$. With the accuracy of our calculations the parameters a, b , and c of this fit do not change with R , while the parameter d is roughly $R + \eta$. Clearly, with an increased accuracy of calculations we may eventually find some dependence of a, b, c on R , but with our current accuracy it appears that $\bar{\phi}^\delta(r)$ has an universal shape independent on R . Undoubtedly, the calculation of $\bar{\phi}^\delta(r)$ will constitute the most time consuming procedure in applying our model to real life problems. It takes about 24 hours to obtain one value of $\bar{\phi}^\delta(r)$ (one point in Fig.2) on a Dell/Pentium4/3Ghz/512Mb computer.

Figure 3 presents typical shapes of the potentials $\phi_b(r)$ (lower solid curve), $\bar{\phi}^\delta(r)$ (upper solid curve), and $\psi_b(r)$ (dashed curve) for a hydrophobic bead around the cluster as functions of the distance r from the center of the cluster of radius $R = 3\eta$. The potential $\phi_i(r)$ is due to the pairwise interactions of the Lennard-Jones type, and has a shape reminiscent thereof. Previous applications²⁰⁻²⁵ of the mean first passage time analysis to nucleation had invariably lead to this kind of the potential well around the cluster.

The average dihedral potential (assigned to a selected bead) $\bar{\phi}^\delta(r)$ has a maximum value at the cluster surface and decreases monotonically with increasing r until it becomes constant for $r \geq \tilde{r}$ which is the maximum distance between beads 1 and 6 (or beads 1 and 7) dependent on R, η , and Θ_0 :

$$\tilde{r} = R + \eta \left(1 + \sqrt{3 - 2 \cos \Theta_0 + 2\sqrt{2(1 - \cos \Theta_0)} \sin \frac{\Theta_0}{2}} \right).$$

Such a behavior of $\bar{\phi}^\delta(r)$ can be thought of as a consequence of an increase in the entropy of the heteropolymer chain as the selected bead 1 approaches the cluster surface for $r < r'$ which occurs because the configurational space available for the neighboring beads (2 through 7) becomes more and more restricted. Once r becomes greater than r' , this piece of the heteropolymer chain (beads 1 through 7) does not feel the presence of the cluster any more. With some degree of liberty $\bar{\phi}^\delta(r)$ can be interpreted as a constrained (with bead 1 fixed) free energy of that piece of the heteropolymer which includes beads 1 through 7.

As a result of the combination of $\phi_b(r)$ and $\bar{\phi}^\delta(r)$ the overall potential $\psi_b(r)$ has a double well shape: the inner well is separated by the potential barrier from the outer well. The geometric characteristics of the wells (widths, depths, etc...) and the height and location of the barrier between them are determined by the interaction parameters $\epsilon_b, \epsilon_l, \epsilon_\delta$. For example, the larger the ratio $\epsilon_\delta/\epsilon_b$, the higher the barrier between the well, the wider the i.p.w. and the narrower the o.p.w. Note that the barrier has different heights for beads in the i.p.w. and o.p.w. The outer boundary of the o.p.w. is due to the confining potential arising because all residues around the cluster are successively linked and are bound thereto. Hence they are confined within some volume wherein the protein is encompassed and the location r_{cf} of the confining potential is assumed to coincide with its outer boundary. For a given N_0 the location r_{cf} is determined by the size of the cluster and densities ρ_f and ρ_u . The existence of the o.p.w. allows one to consider the absorption of a bead by the cluster as an escape of the bead from the o.p.w. by crossing over the

barrier into the i.p.w. This makes it possible to use the mean first passage time analysis for the determination of the rate of absorption of beads by the cluster. Since the use of the traditional expression for the absorption rate (based on the gas-kinetic theory)⁴⁶ is rather inadequate in the cluster growth within the protein, the double-well shape of $\psi_i(r)$ is of crucial importance to our model for the nucleation mechanism of protein folding.

Figure 4 presents W^- and W^+ , the emission and absorption rates, respectively, as functions of the cluster size R . The location of the intersection of these functions determines the size of the critical cluster, R_c . The emission rate is greater than the absorption rate, $W^-(r) > W^+(r)$, for small clusters with $R < R_c$, whereas for clusters larger than the nucleus the absorption dominates over the emission, $W^-(r) < W^+(r)$ for $R > R_c$. Note that both W^- and W^+ increase with increasing R , but W^- increases roughly linearly with R whereas W^+ shoots up by several orders of magnitude after the cluster becomes supercritical. This is a consequence of the fact that the width of the o.p.w. quickly decreases as the cluster grows while the outer height of the barrier between the i.p.w. and o.p.w. does not virtually change, and it becomes increasingly easy for a bead which is in the o.p.w. to cross over the barrier and fall into the i.p.w.

The behaviour of W^- and W^+ also explains our numerical estimates for the characteristic times of the first nucleation event t_n , growth time t_g , and total folding time t_f by eqs.(32),(33), and (35). Although these depend very much on the location of R_c and the value of D_{iw} (R_c itself does not depend on D_{iw} but only on the ratio D_{ow}/D_{iw}), always $t_n \gg t_g$, i.e., the protein folding time is mainly determined by the time necessary for the first nucleation event. Physically, this is the case because the increase of the cluster size from $\nu = 1$ to $\nu = \nu_c$ occurs only owing to fluctuations which have to overcome the natural tendency of a small cluster to decay ($W^+ < W^-$ for $\nu < \nu_c$). For supercritical clusters W^+ so quickly immensely overwhelms W^- that fluctuations are unable to impede the natural tendency of the cluster to grow (strictly speaking, this is true only for $\nu > \nu_c + \Delta\nu_c$, but for rough estimates eq.(35) is acceptable). For the above choice of system parameter and D_{iw} in the range from 10^{-6} cm²/s to 10^{-8} cm²/s our model predicts the characteristic time of the protein folding (for $N_0 = 2500$) in the range from several seconds to several hundreds of seconds which is in a very good agreement with expectations based on experimental data.

5 Conclusions

So far most of the work on the protein folding has been done by using either Monte Carlo (MC) or molecular dynamics (MD) simulations. The rigorous theoretical treatment of the protein folding by means of the statistical mechanics is hardly practicable because of the extreme complexity of the system. A number of simulations have suggested that there can exist multiple pathways for a protein to fold one of which has been identified as reminiscent of nucleation. However, a theoretical model for the nucleation mechanism of the process had so far remained underdeveloped. The previous model, based on the approach of the classical nucleation theory (CNT), was a purely thermodynamic one considered the formation of a cluster of protein residues and calculated the free energy change thereupon.^{14,18} The number of a critical cluster (nucleus) was provided by the location of the maximum of the free energy of formation as a function of a single independent variable of state of the cluster. In such a model the free energy of cluster formation depends on the surface tension of a cluster of protein residues. This quantity is an ill-defined physical quantity and can be considered only as an adjustable parameter. According to the nucleation mechanism,

after the formation of the nucleus (critical size cluster of residues), the protein quickly reaches its native state.

In the present work we present a new, microscopic model for the nucleation mechanism of the protein folding. A protein is considered as a heteropolymer consisting of two type of beads (hydrophobic and hydrophilic) linked with bonds of fixed length. All bond angles are also assumed to be fixed and equal to 105° . All non-adjacent beads are assumed to interact via Lennard-Jones like potential. Besides these interactions, the total energy of the heteropolymer contains a contribution from dihedral angles of all triads of successive links. Unlike the old model, ours is developed without recurring to CNT approach. Instead, it is based on the above “molecular” interactions, both long-range and configurational. The parameters of these potentials can be rigorously defined, unlike the ill-defined surface tension of a cluster of protein residues.

The crucial idea underlying the new model consists of averaging the dihedral potential in which a selected residues is involved over all the possible configurations of neighboring residues. The resulting average dihedral potential depends on the distance between the residues and the cluster center. It has a maximum at the cluster surface and monotonically decreases with increasing distance therefrom. Its combination with the average potential due to pairwise interactions between the selected residue and those in the cluster a double potential well around the cluster with a barrier between the two wells. Residues in the inner well are considered to belong to the cluster (part of the protein with correct tertiary contacts) while those in the outer well are treated as belonging to the mother phase (amorphous part of the protein with incorrect tertiary contacts). Transitions of residues from the inner well into the outer one and vice versa are considered as elementary emission and absorption events, respectively. The rates of these processes are determined by using the mean first passage time analysis. Once these rates are found as functions of the cluster size, one can develop a self-consistent kinetic theory for the nucleation mechanism of protein folding. For example, the size of the critical cluster (nucleus) is then found as the one for which these rates are equal. The time necessary for the protein to fold can be evaluated as a sum of the times necessary for the appearance of the first nucleus and the time necessary for the nucleus to grow to the maximum size (of the folded protein in the native state).

For numerical illustration we have considered a model protein consisting of 2500 beads with the mole fraction of hydrophobic beads equal to 0.75. The composition of the cluster during its formation and growth was assumed to be constant and equal to the composition of the whole protein. This allows one to consider the model as a single component one. The size of the critical cluster and the folding time predicted by the model depend very much on many parameters of the system, such as interaction parameters, densities of the protein in the unfolded (but compact) and folded states, diffusion coefficients therein, etc. With an appropriate choice of interaction parameters and densities, the size of the critical cluster predicted by our model is about 220 residues and with the free energy of nucleus formation being about $20k_BT$. This results suggest that the quantity equivalent to the “surface tension” in the old model of nucleation in a protein, should be smaller than the previous estimates^{14,18} of the latter by an order of magnitude. The characteristic time of protein folding was estimated to be in the range from several seconds to several hundreds of seconds depending on the diffusion coefficient of native residues in the range $10^{-6} \text{ cm}^2/\text{s}$ to $10^{-8} \text{ cm}^2/\text{s}$. This is consistent with experimental data⁵⁵ on typical folding times of proteins as well as with estimates obtained by other theoretical models¹⁸ and in simulations.^{6,14}

A further development of our model will require the removal of several simplifying assumptions that we recurred to in the present work. For example, it would be more appropriate to model a protein as a three-component heteropolymer (including not only hydrophobic and hydrophilic

residues, but also neutral ones). This will result in more lengthy numerical calculations of the average dihedral potential because the dihedral potential involving neutral beads is expected to be lower and requires separate calculations. Next, the cluster composition during its formation and growth can quite significantly depend on the cluster size, particularly in the vicinity of the critical size, so assuming it constant in the present work might have lead to serious inaccuracy in the results. Including neutral beads in the model and allowing the cluster composition to differ from that of the protein will result in a binary or even ternary nucleation mechanism of protein folding. However, besides some increase in computational efforts there seem to exist no principal difficulty in developing the model in these directions. Some other improvements of the model can be also introduced in the model, but they will be discussed in our future papers on the subject.

Acknowledgments - I am grateful to Professors F.M.Kuni, A.P.Grinin, and E.Ruckenstein for many helpful discussions of this work which was supported by the National Science Foundation through the grant CTS-0000548.

References

¹T.E.Creighton, in *Proteins: Structure and Molecular Properties*, edited by W.H.Freeman (San Francisco, 1984)

²L.Stryer, in *Biochemistry*, edited by W.H.Freeman (1988).

³C.Ghelis and J.Yan, *Protein Folding* (Academic Press, New York,1982).

⁴C.B.Anfinsen, *Science* **181**, 223-230 (1973).

⁵J.D.Honeycutt and D.Thirumalai, *Proc.Natl.Acad.Sci. USA* **87**, 3526-3529 (1990).

⁶J.D.Honeycutt and D.Thirumalai, *Biopolymers* **32**, 695-709 (1992).

⁷J.S.Weissman and P.S.Kim, *Science* **253**, 1386-1393 (1991) .

⁸T.E.Creighton, *Nature (London)* **356**, 194-195 (1992).

⁹P.S.Kim and R.I.Baldwin, *Annu.Rev.Biochem.* **51**, 459 (1982).

¹⁰P.S.Kim and R.I.Baldwin, *Annu.Rev.Biochem.* **59**, 631 (1990).

¹¹T.E.Creighton, *Biochem. J.* **240**, 1 (1990).

¹²T.E.Creighton, *Prog.Biophys.Mol.Biol.* **33**, 231 (1978).

¹³Z.Guo, D.Thirumalai, and J.D.Honeycutt, *J.Chem.Phys.* **97**, 525-535 (1992).

¹⁴Z.Guo and D.Thirumalai, *Biopolymers* **36**, 83-102 (1995).

¹⁵D.Thirumalai and Z. Guo, *Biopolymers* **35**, 137-140 (1995).

¹⁶J.D.Bryngelson and P.G. Wolynes, *Proc.Natl.Acad.Sci.(USA)* **84**, 7524 (1987); *J.Phys.Chem.* **93**, 6902 (1998).

¹⁷E.I.Shakhnovich and A.M.Gutin, *Nature* **346**, 773 (1990); *J.Phys.A* **22**, 1647 (1989).

¹⁸J.D.Bryngelson and P.G.Wolynes, *Biopolymers* **30**, 177 (1990).

¹⁹K.A.Dill, *Biochemistry* **24**, 1501 (1985); **29**, 7133 (1990).

²⁰G.Narsimhan and E. Ruckenstein, *J. Colloid Interface Sci.* **128**, 549 (1989).

²¹E.Ruckenstein and B. Nowakowski, *J. Colloid Interface Sci.* **137**, 583 (1990).

²²B.Nowakowski and E. Ruckenstein, *J. Colloid Interface Sci.* **139**, 500 (1990).

²³Y.S.Djikaev and E.Ruckenstein, *J.Chem.Phys.* **123**, 214503 (2005).

²⁴Y.S.Djikaev and E.Ruckenstein, *J.Chem.Phys.* **124**, 124521 (2006).

²⁵Y.S.Djikaev and E.Ruckenstein, *J.Chem.Phys.* **124**, 124521 (2006).

²⁶M.Levitt and R. Sharon, *Proc.Natl.Acad.Sci.USA* **85**, 8557 (1988).

²⁷J.Skolnik, A. Kolinski, and R. Yaris, *Biopolymers* **28**, 1058 (1989).

²⁸A.Kolinski, J. Skolnik, and R. Yaris, *Biopolymers* **26**, 937 (1987).

²⁹A.Sikorski and J. Skolnik, *Biopolymers* **28**, 1097 (1989); *ibid* *J.Mol.Biol.* **213**, 183 (1990).

³⁰J.Skolnik and A. Kolinski, *Science* **250**, 1121 (1990).

³¹C.Levinthal, in *Mössbauer Spectroscopy in Biological Systems*, edited by P.Debrunner, J.C.M.Tsibris and E.Mönck, (University of Illinois Press, 1968).

³²D.Wetlaufer, *Proc.Natl.Acad.Sci. USA* **70**, 697 (1973).

³³T.Y.Tsong, R.Baldwin, and P.McPhie, *J.Mol.Biol.* **63**, 453 (1972).

³⁴J.Moult and R.Unger, *Biochemistry* **30**, 3816 (1991).

³⁵K.Dill, K.Fiebig, and H.S.Chan, *Proc.Natl.Acad.Sci.USA* **90**, 1942 (1993).

³⁶D.J.Lee, M. M. Telo da Gama, and K. E. Gubbins, *J. Chem. Phys.* **85**, 490 (1986).

³⁷A.I.Rusanov, *Phasengleichgewichte und Grenzflachenerscheinungen* (Academie, Berlin, 1978).

³⁸R.C.Tolman, *J. Chem. Phys.*, **17**, 333 (1949).

³⁹J.G.Kirkwood and F.P. Buff, *J. Chem. Phys.*, **17**, 338 (1949).

⁴⁰C.Flageollet, M. Dihn Cao, and P. Mirabel, *J. Chem. Phys.* **72**, 544 (1980).

⁴¹G.Wilemski, *J. Phys. Chem.* **91**, 2492 (1987).

⁴²B.E.Wyslouzil, J. H. Seinfeld, R. C. Flagan, and K. Okuyama, *J. Chem. Phys.* **94**, 6827 (1991).

⁴³A.Laaksonen, *J. Chem. Phys.* **97**, 1983 (1992).

⁴⁴G.Wilemski, *J. Chem. Phys.* **80**, 1370 (1984).

⁴⁵Y.S.Djikaev, I. Napari, A. Laaksonen, *J. Chem. Phys.* **120**, 9752 (2004).

⁴⁶F.F.Abraham, *Homogeneous Nucleation Theory* (Academic, New York, 1974).

⁴⁷S.Chandrasekhar, *Rev. Mod. Phys.*, **15** (1949) 1.

⁴⁸C.W. Gardiner, *Handbook of Stochastic Methods* (Springer, New York/Berlin, 1983).

⁴⁹N.Agmon, *J. Chem. Phys.*, **81**, 3644 (1984).

⁵⁰J.Lothe and G. M. J. Pound, In *Nucleation*, edited by A. C. Zettlemoyer (Marcel-Dekker, New York, 1969).

⁵¹J.Schmelzer, G. Röpke, and V. B. Priezzhev, Eds. *Nucleation Theory and Applications* (JINR, Dubna, 1999).

⁵²D.Kashchiev, *Nucleation: Basic Theory with Applications* (Butterworth-Heinemann, Oxford, 2000).

⁵³Y.Harpaz, M.Gerstein, and C.Chothia, *Structure*, **2**, 641-649 (1994).

⁵⁴D.M.Huang and D.Chandler, *Proc.Natl.Acad.Sci.USA*, **15**, 8324-8327 (2000).

⁵⁵B.Nötling, *Protein Folding Kinetics* (Springer-Verlag, Berlin, 2006).

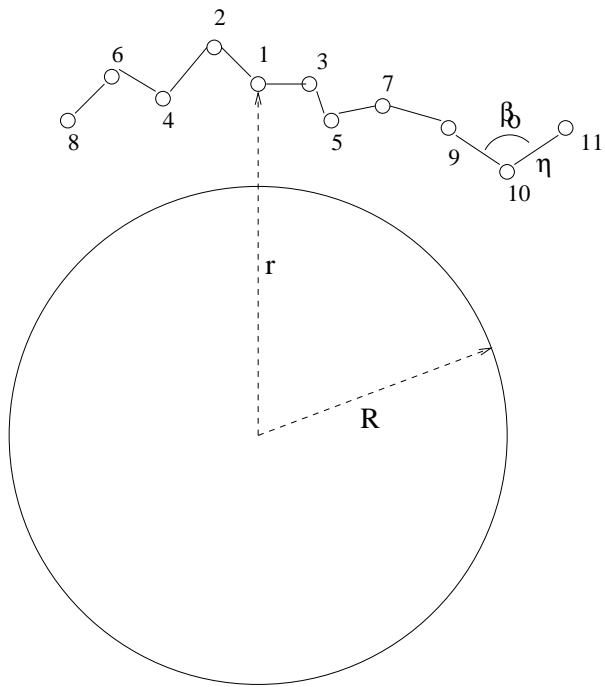


Figure 1: A scheme of a piece of a heteropolymer chain around the spherical cluster (shown only partly) of radius R . Bead 1 lies in the Figure plane, whereas beads 2 through 7 may all lie in different planes, but all bond angles are equal to 105° and their lengths are equal to η . The distance between the selected bead 1 and the center of the cluster is r

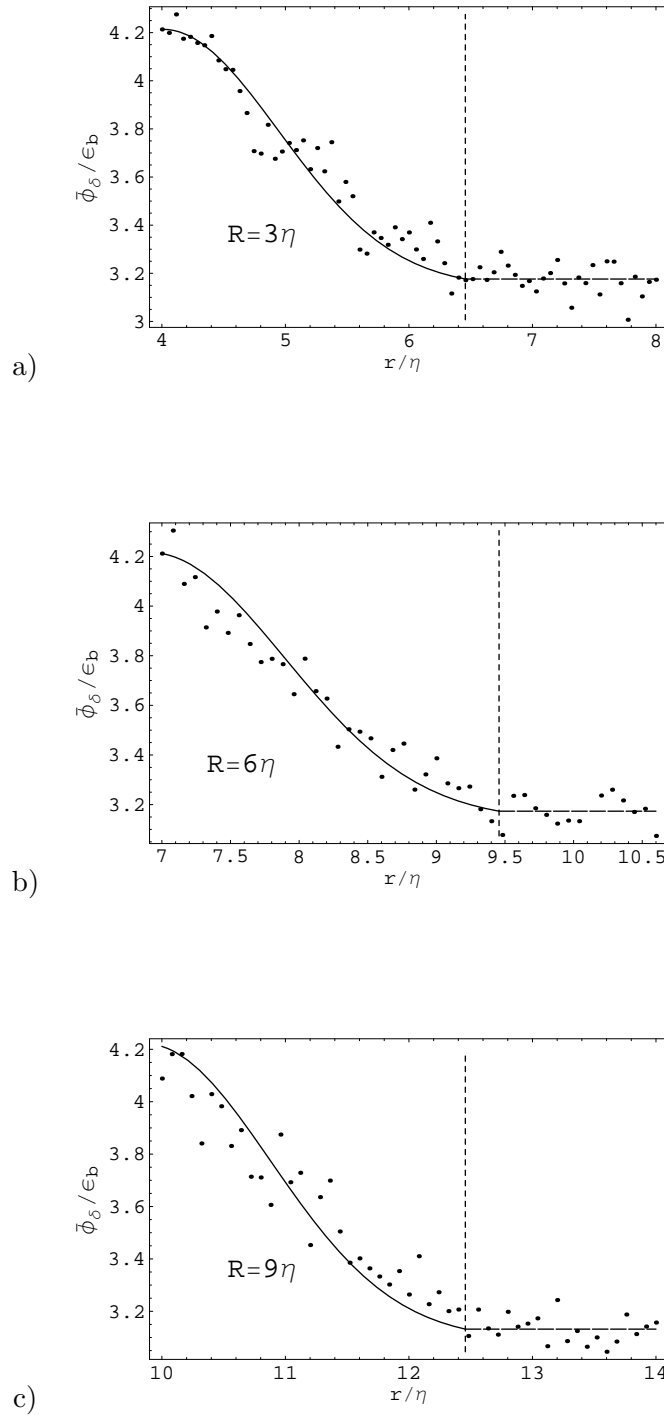


Figure 2: The average dihedral potential (assigned to a selected bead) $\bar{\phi}_\delta(r)$ as a function of r for three clusters of sizes (a) $R = 3\eta$, (b) $R = 6\eta$, and (c) $R = 9\eta$. The points represent the actual numerical results obtained by using the Monte Carlo integration in eqs.(21),(22). The vertical dashed lines correspond to \tilde{r} . The solid lines are analytic fits by an expression $a + b \exp[-c(r - d)^2]$.

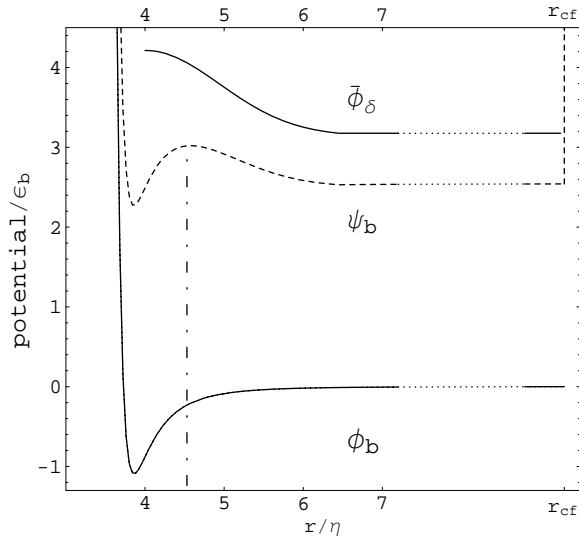


Figure 3: Typical shapes of the potentials $\phi_b(r)$ (lower solid curve), $\bar{\phi}_\delta(r)$ (upper solid curve), and $\psi_b(r)$ (dashed curve) for a hydrophobic bead around the cluster as functions of the distance r from the center of the cluster of radius $R = 3\eta$. The outer boundary of the o.p.w. ($r_{cf} \simeq 12.99\eta$) was assumed to coincide with the outer boundary of the volume wherein the whole protein is encompassed.

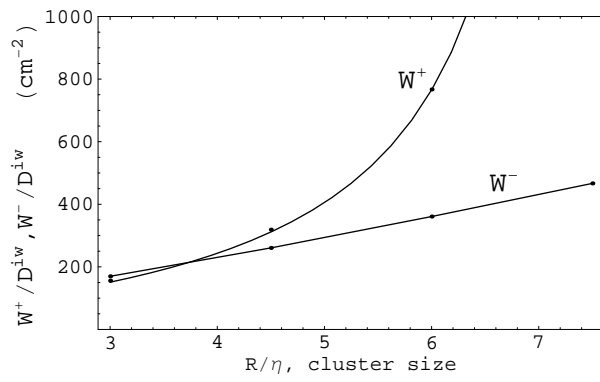


Figure 4: Figure 4 presents W^- and W^+ , the emission and absorption rates, respectively, as functions of the cluster size R . The location of the intersection of these functions determines the size of the critical cluster, R_c